DISCRIMINATION OF TSUNAMI SOURCES (EARTHQUAKE VS. LANDSLIDE) ON THE BASIS OF HISTORICAL DATA IN EASTERN SICILY AND SOUTHERN CALABRIA

Flavia Gerardi*, Maria Serafina Barbano
Dipartimento di Scienze Geologiche, Università di Catania, Corso Italia 55, 95129 Catania, Italy
Paolo Marco De Martini, Daniela Pantosti
Istituto Nazionale di Geofisica e Vulcanologia, Sezione Sismologia e Tettonofisica, Via di Vigna Murata 605, 00143 Roma, Italy

*Corresponding author. Phone: +39-095-7195729; Fax: +39-095-7195712.
E-mail addresses: f.gerardi@unict.it (F. Gerardi), barbano@unict.it (M.S. Barbano), demartini@ingv.it (P.M. De Martini), pantosti@ingv.it (D. Pantosti)

Abstract

The source mechanisms responsible for large historical tsunamis that have struck eastern Sicily and southern Calabria are a topic of robust debate. We have compiled a database of historical coeval descriptions of three large tsunamis: 11 January 1693, 6 February 1783 and 28 December 1908. By using accounts of run-up and inundation and employing an approach proposed by Okal and Synolakis, in 2004, we can provide discriminants to define the nature of the near-field tsunami sources (fault dislocation or landslide).

Historical reports for the 1908 event describe affected localities, maximum run-ups and inundation areas. However, for the 1693 and 1783 tsunamis, reports are limited to inundation and occasional run-up estimates. We calculate run-up values for these events using available relations between inundation and run-up. We employed the model of Okal and Synolakis to the obtained profiles of tsunami run-up along the inundated shorelines. The 1908 run-up data distribution confirms that the tsunami is compatible with a seismic dislocation source, whereas the 1783 data supports contemporary observations and recent offshore investigations suggesting that the tsunami was produced by an earthquake-triggered submarine landslide. Analysis of the 1693 event data suggests that tsunami was generated during a tectonic event and thus a seismogenic source should be found offshore.

Keywords: historical earthquakes; tsunami; run-up; seismic dislocations; landslides; southern Italy

1. Introduction

Coastal areas of southern Calabria and eastern Sicily have been affected by large destructive earthquake-related tsunamis in historical times. As described in contemporary reports, devastating waves followed the 11 January 1693, 6 February 1783 and 28 December 1908 earthquakes (Fig. 1). Despite the dramatic impact of these earthquakes in the region, there is little consensus concerning their causative faults; thus several hypotheses of faults/seismic sources exist in the literature (e.g. Ghisetti, 1992; Valensise and Pantosti, 1992; Jacques et al., 2001; Galli and Bosi, 2002; Monaco and Tortorici, 2000; DISS Working Group, 2006 and references therein). Moreover, for the 1693 event, both offshore and inland source locations have been suggested (D'Addezio and Valensise, 1991; Sirovich and Pettenati, 1999; Azzaro and Barbano, 2000; Jacques et al., 2001; Gutscher et al., 2006; DISS Working Group, 2006; Basili et al., 2008). Uncertainties in the locations of these earthquake sources have generated discussion about the origin of the tsunamis and, in particular, whether they were related to a seismic dislocation or to a submarine landslide (e.g. Tinti and Armigliato, 2003; Tinti et al. 2007; Billi et al., 2008).

The objective of this paper is to discriminate among the possible sources of tsunamis by using run-up amplitudes observed in the near-field and by applying a method proposed by Okal and Synolakis (2004) to the 11 Jan 1693, 6 Feb 1783 and 28 Dec 1908 tsunamis. On the basis of tsunami numerical run-up simulations performed for several different seismic dislocation and landslide source models, Okal and Synolakis (2004) reported that run-up height distribution and length of inundated shorelines might vary depending on the type of tsunami source (earthquake or landslide). The Okal and Sinolakis (2004) approach was initially developed for a rectilinear coastline and for open oceans. Nonetheless, we believe it also can be applied to the southern Calabria and eastern Sicilian coasts because: (1) the method is for near-field tsunamis; (2) although the Ionian basin (1000-3000 m) is not as deep as oceanic depths the impact of depth on the model is negligible within the results as demonstrated by Okal and Sinolakis (2004); and (3) most of the coastline affected by the tsunamis fits the condition of an approximately straight line with exception of the narrower part of Messina Straits.

We compiled a database of known tsunami inundation and run-up observations from eastern Sicily and southern Calabria with the aim of reconstructing run-up distribution. This database has been assembled through an intensive search of historical reports (Boschi et al., 2000; Tinti et al., 2004) and seismological compilations such as Perrey (1848), De Rossi (1889), Mercalli (1897) and Baratta (1901). Additional sources, mainly newspapers and local chronicles, have also been analyzed. In the following chapter, we summarize the present knowledge of the 11 Jan 1693, 6 Feb 1783, and 28 Dec 1908 earthquake sources and the historical data available for each associated tsunami.

2. Earthquake sources and tsunamis

2.1 January 11, 1693

The M_{aw} = 7.4 1693 earthquake (hereinafter M_{aw} = equivalent moment magnitude from macroseismic data according to Working Group CPTI, 2004) caused destruction and extensive damage in most localities of eastern Sicily (Boschi et al., 2000). The location of this earthquake source is still unknown. It affected large coastal areas and was preceded by a strong foreshock two days earlier (Barbano and Cosentino, 1981; Boschi et al., 2000). Hypothesized possible sources vary considerably (e.g. D'Addezio and Valensise, 1991; Sirovich and Pettenati, 1999; Azzaro and Barbano, 2000; Gutscher et al., 2006; DISS Working Group, 2006 and references therein), ranging from an offshore fault to an inland source (Fig. 1). Inland source models, based on geologic, geomorphic or macroseismic intensity analyses, depict either a normal fault within the Scordia-Lentini graben (L1 or L2 in Fig.1, D'Addezio and Valensise, 1991, Tinti and Armigliato, 2003) or a blind strike slip fault, parallel to the Scicli line (SL in Fig.1, Sirovich and Pettenati, 1999; or RF in Fig.1, DISS Working Group, 2006). Offshore source models, based on tectonics, analysis of seismic prospecting data, and tsunami modeling suggest the rupture of a segment of the Malta escarpment (ME in Fig.1, Piatanesi and Tinti, 1998; Azzaro and Barbano, 2000; Jacques et al., 2001; Argnani and Bonazzi, 2005) or of a subduction zone fault (SZ in Fig. 1, Gutscher et al., 2006).

Following the earthquake, a large tsunami struck the entire eastern coast of Sicily, the Aeolian Islands and the old Port of Marina di Ragusa, Mazzarelli (Campis, 1694), on the southern Sicilian coast (Fig. 2). The known length of inundated shoreline was about 230 km. The sea withdrew ~ 100 m and returned back to overflow the dock at the Messina harbor (Anonymous, 1693). The largest inundation is described at Mascali, where the sea flooded the shore for about ~ 1.5 km inland (Boccone, 1697). San Filippo square (now Mazzini square) in Catania and the farmlands around the city (Boccone, 1697) were submerged. The most affected location was the town of Augusta, where the sea withdrew completely from the harbor and then violently returned to flood the coast ~ 165 m inland (Bottone, 1718). Moreover, sea level rose ~ 2.40 m inundating the town as far as the San Domenico Monastery (Boccone, 1697). According to another report the run-up reached 8 m (ASV, 1693).

Explaining the size and extent of this tsunami without the rupture of a major offshore or coastal fault is difficult. However, Tinti et al. (2007) model a 5 km^3 landslide offshore from Augusta (Fig. 2) as a possible source.

2.2 February 6, 1783

The 1783 seismic sequence was comprised of 5 strong shocks that occurred between February and March (Fig. 1) and ruined many towns in Calabria and north-eastern Sicily (Boschi et al., 2000). Tsunamis were observed after the two shocks of 5 February (M_{aw} = 6.9) and 6 February (M_{aw} = 5.9) (Working Group CPTI, 2004). Although data for the 5 Feb tsunami are scanty and generic (e.g. “considerable sea withdrawal”, “the sea surpassed the beach”, “buildings along the shore were violently inundated”, Sarconi, 1784), it is possible to separate the effects of the two tsunamis on the affected locations from the overall historical descriptions (Graziani et al., 2006). The 6 February tsunami affected the Sicilian coast from Messina to Torre Faro and the Calabrian coast from Reggio Calabria to Scilla (Fig. 3) for a total length of 40 km. The highest tsunami wave was about 16 m high. It struck Scilla killing 1500 people, who had fled to the beach to escape the earthquake's destruction in the town. The wave flooded ~ 170 m into the Livorno stream valley, near Scilla (Vivenzio, 1783). At Torre Faro, the tsunami wave flooded the shore, extending ~ 400 m inland depositing a large amount of silt and numerous dead fish (Sarconi, 1784). In Messina, the sea rose about 2 m and reached the fish-market killing 28 people (Vivenzio, 1783; Spallanzani, 1795).

The source of the 6 February 1783 earthquake has been identified as the Scilla fault (SF in Fig. 1, Jacques et al., 2001). Although the associated tsunami could have been caused by fault slip, a 16 m wave from a M_{aw} = 5.9 event is unlikely. Moreover, historical accounts report that the earthquake triggered a huge rock-fall along the western cliff of the Mount Campallà at Scilla that fell into the sea, thereby generating a disastrous tsunami (Minasi, 1785). A recent geophysical survey offshore from Scilla shows a large submarine landslide. Bosman et al. (2006) and Bozzano et al. (2006) hypothesize kinematic relations between the submarine and sub aerial features have been suggested.

2.3 December 28, 1908

The 28 December 1908 Messina earthquake (M_w= 7.1, Pino et al., 2000) was the most catastrophic natural disaster of the 20th century in Italy. It produced extensive destruction over an area embracing southern Calabria and north-eastern Sicily (Boschi et al., 2000). The earthquake, tsunami, and fires destroyed about 90% of the existing buildings in Messina and Reggio Calabria, killing more than 80,000 people (Mercalli, 1909). The earthquake source, located in the Messina Straits, is not clearly identified. It is depicted variously as a west dipping normal fault (M1 in Fig. 1) (Ghisetti, 1992; Jacques et al., 2001), or a blind, east-dipping, low-angle, normal fault, with a minor strike-slip component (M2 in Fig. 1) (Valensise and Pantosti, 1992; Pino et al. 2000; DISS Working Group, 2006).

The tsunami reached the southern Calabrian (Fig. 4a, b) and eastern Sicilian coasts (Fig. 4c, d) a few minutes after the earthquake, causing further damage and casualties (Platania, 1909; Sabatini, 1910). Tsunami effects were also observed along the Tyrrhenian coast of Sicily as far as Termini Imerese, and in the Sicily Channel at Licata and Malta Islands (Fig.1), where the sea level rose more than 1 m (Platania, 1909; Baratta, 1910). The maximum run-up elevation along the Calabrian side of Messina Straits was about 10 m, near Lazzaro (Fig. 4a) (Baratta, 1910). The waves flooded the Chiesa della Marina at Gallico (Fig. 4b), near the railway station at a distance of about 375 m inland from the present shore-line (Baratta, 1910).

In Sicily, run-up in Messina near the harbor office, in Vittorio Emanuele Street, and near the St. Salvatore fortress was about 3 m, and about 6 m at the mouth of the Portalegni stream (Fig. 4c) (Platania, 1909). The tsunami inundated the city of Catania for more than 100 m inland (Fig. 4d) depositing algae, posidonie, madrepore and millepore fragments, mollusks and many dead fish. The shore was flooded about 700 m inland at the mouth of the Simeto River (Baratta, 1910). The southernmost locality affected by the tsunami was Capo Passero (Fig.4c), where a run-up of 1.5 m was observed (Platania, 1909). The tsunami reached its maximum run-up along the northeastern Sicilian coast at Capo S. Alessio (Fig. 4c) where a run-up of 11.7 m was measured (Platania, 1909).

3. Run-up estimation

In order to discriminate between the type of tsunami sources using the method of Okal and Synolakis (2004), run-up values at different locations are needed. With the exception of the 1908 tsunami, data are limited and mainly comprise inundation records (Fig. 2 and 3).

The following equation (Hills and Mader, 1997) is used to convert inundation data to run-up values:

$$x_{max} = (H_s)^{1.33}\, n^{-2}\, k \quad (1)$$

where x_{max} = limit of landward incursion (inundation, m); H_s = run-up (m); k = a constant (0.06). Roughness of the surface of the land is represented by Manning's coefficient *n* that is 0.015 for very smooth topography, 0.03 for urbanized/built land, and 0.07 for densely forested landscape. Run-up at a single location along an actual shore is affected by other local factors such as shore slope and presence of bays, estuaries and shoreline protuberances. We consider this equation to be best suited for flat coastal areas consistent with most of the sites for which observed run-up data are available.

The wealth of information for the 1908 tsunami (more than 25 sites where both run-up and inundation were observed) offers a unique opportunity to use the historical data to define Manning's coefficient *n* for the landscape present in southern Calabria and eastern Sicily. First, we fit the 1908 run-up and inundation data into the equation (1) (diamonds in Fig. 5). This procedure provides a best fit value for $n = 0.06$, with most values in the range $n = 0.04$ and 0.09. Then, we compute run-up values (triangles in Fig. 5) from observed inundations using different values of Manning's *n* to define the best value for each 1908 site using equation (1). Because observed and computed run-up values are in good agreement, we can use the Hills and Mader (1997) equation for those locations affected by the 1693 and 1783 tsunamis. The *n* values obtained for each of these locations (Table 1) are used in order to predict run-ups (grey values in Figs. 2 and 3) from inundations. Furthermore, to take into account the possible uncertainty associated with our estimates, we also computed run-ups for all locations by using the end values for the whole 1693 and 1783 dataset ($n = 0.03$ and 0.07, Table 1). This provided a range between maximum and minimum possible run-ups for the 1693 and 1783 events (grey values in parentheses in Figs. 2 and 3).

Testing the results obtained for the 1693 and 1783 tsunamis against their limited available run-up values, the calculated run-ups estimates agree with observed ones. For example, in the town of Augusta (Fig. 2) historical sources provide two different run–up values for the 1693 tsunami: Boccone (1697) reports “le acque alzaronsi più dell’ordinario livello quasi otto piedi geometrici” (the waters rose above the usual sea level by 8 geometrical feet [~ 2.4 m]); whereas according to the ASV (1693) “il mare si alzò dalla solita riva di quattro canne” (the sea rose from its natural shoreline by 4 “canne” [~ 8 m]). In addition, inundation in Augusta is described by Bottone (1718): “Il mare si gonfiò di trenta cubiti oltre il solito limite” (the sea grew by 30 cubits [~ 165 m], beyond the usual shoreline). Thus, by introducing the inundation value of 165 m into equation (1), we obtain run-up values of 2 and 7 m for n = 0.03 and n = 0.07, respectively (Fig. 2). This is in good agreement with the few observed values. Moreover, the observed run-ups in Messina (~ 2 m) and Marina di Scilla (~7 m) for the 6 February 1783 tsunami (Fig. 3), are within the range of the computed run-up values from inundations (0.8 - 2.3 m and 2.3 – 8 m, respectively). These comparisons support the strength of run-up estimate from inundation data.

4. Landslide vs. dislocation

In an attempt to discriminate the physical nature of the 1908, 1783, and 1693 tsunami sources, we used different distributions of run-up amplitudes (observed or derived from Hills and Mader, 1997) along a defined stretch of coastline and applied the method described by Okal and Synolakis (2004). For each event, we simplified the actual coastline, by constructing a coastal profile using straight line segments that approximate the variability of the coast, and projected the run-up observed at individual locations onto these segments. The origin of the tsunami relative to the profile is set at the nearest point with respect to the tsunami source. We use historical and computed run-up values and different idealized linear profiles to account for the varied orientations of the Calabrian and Sicilian coasts around the Messina Straits. Here, we present only the boundary results derived from this analysis.

For the 1908 tsunami, we set the source within the Messina Straits at the latitude of Reggio Calabria and constructed three idealized profiles: one fits the Calabrian coast (Fig. 6a inset), another the Sicilian coast (Fig. 6b inset), and the third incorporates both coasts (Fig. 6c inset).

For the 6 February 1783 event, we set the tsunami source near Scilla and construct two profiles with different orientations (N10°E Fig. 7 a, b and c and N35°E, Fig. 7 d, e and f, see inset map), and run-ups computed with different Manning *n* values (Table 1). Since the run-up values are mostly derived from inundation observations, to include all the uncertainties, we also plotted run-ups computed with $n = 0.07$ (maximum run-ups) and with $n = 0.03$ (minimum run-ups), obtaining on the whole three different run-up profiles for each orientation.

For the 1693 tsunami, we set the 0 point (hypothesized source position) between Catania and Augusta and plot the run-up values along one coastline profile (inset of Fig. 8). We use run-ups (Fig. 8a) obtained from inundation data using varied Manning *n* values (Table 1) and also utilize maximum and minimum run-up values obtained from $n = 0.07$ and 0.03 (Fig. 8b and c, respectively), getting three different run-up profiles.

For each event, we empirically estimate the best fit of the different run-up distributions along the coastline profiles using the formula proposed by Okal and Synolakis (2004):

$$\zeta(y) = b / \{[(y-c)/a]^2 + 1\} \quad (2)$$

where ζ is the run-up at each point y, “a” is the lateral extent of sustained run-up along the coastline profile, “b” is the maximum amplitude run-up on the fitted curve and “c” is the distance of “b” from 0 (the tsunami origin), along the idealized linear profile.

We calculated several sets of parameters (a, b, c) for equation (2) in order to find the theoretical best-fit curve of historical and computed run-up values (Fig. 6, 7, 8), i.e., the curve that gives the smallest RMS with the point distribution. Therefore, for each run-up distribution along individual coastline profiles, a set of a, b, c parameters is obtained.

Note the different behavior of the 1783 run-up distributions along the coast with respect to 1693 and 1908. On average, “b” values, namely the maximum amplitude run-up on the best fit curves, are smaller for the 1693 and 1908 run-up distributions than for the 1783 event; whereas “a” values, namely the extent of the affected coastline on the best fit curves, are much smaller for the 1783 than for the 1693 and 1908 tsunamis.

The values “a” and “b”, obtained from the different best-fit curves, are used to calculate the dimensionless parameter

$$I_2 = b/a \quad (3)$$

that represents the ratio of the maximum run-up “b” to the characteristic width “a” of its distribution along the beach. According to Okal and Synolakis (2004), I_2 is the discriminating factor for the nature of the tsunami source. They found that an I_2 value smaller than 10^{-4} is characteristic of a seismic dislocation source; whereas, when I_2 is larger than 10^{-4}, the source is likely to be an underwater landslide. Okal and Synolakis (2004) tested the effectiveness of this parameter using observed data from nine worldwide tsunamis.

Using the “a” and “b” values obtained by separating the data recorded along the two sides of the Messina Straits for the 1908 event, we get $I_2 = 4.5 \cdot 10^{-5}$ (a = 115 km and b = 5.25 m), for the Calabria run-up distribution (Fig. 6a) and $I_2 = 6 \cdot 10^{-5}$ (a = 110 km and b = 6.5 m) for eastern Sicily (Fig. 6b). Using data from both coasts yields an $I_2 = 6.3 \cdot 10^{-5}$ (a = 90 km and b = 5.75 m, Fig. 6c). The I_2 values obtained for the 1908 data (I_2 smaller than 10^{-4}) suggest that its source is a fault dislocation. This is in agreement with the tsunami source proposed in the literature for the 1908 event (Piatanesi et al., 1999; Tinti and Armigliato, 2003).

Conversely, for the 1783 tsunami, we obtain $I_2 = 4.33 \cdot 10^{-3}$ (a = 3 km and b = 13 m) for the N10°E profile (Fig. 7a) and $I_2 = 3.6 \cdot 10^{-3}$ (a = 3.75 km and b = 13.5 m) for the N35°E profile (Fig. 7d) using run-up values obtained from inundation data with different Manning *n* values (Table 1). We also calculate I_2 using "a" and "b" values obtained by maximum and minimum run-up distributions, acquired from *n* = 0.07 and 0.03. This yields $I_2 = 4.5 \cdot 10^{-3}$ (a = 3 km and b = 13.5 m) (Fig. 7b) and $I_2 = 3.6 \cdot 10^{-3}$ (a = 2.5 km and b = 9 m) for the N10°E profile (Fig. 7c), and $I_2 = 3.2 \cdot 10^{-3}$ (a = 4 km and b = 13 m) (Fig. 7e) and $I_2 = 3.6 \cdot 10^{-3}$ (a = 3 km and b = 11 m), for the N35°E profile (Fig. 7f). The I_2 values obtained for the 1783 data (I_2 larger than 10^{-4}), suggests that the tsunami source was likely a landslide.

Because the Okal and Synolakis (2004) methodology gives results that agree with previous findings (based on historical and modeling datasets), we applied the same procedure to the 1693 tsunami which has a source type that is a matter of debate.

We calculated $I_2 = 6.6 \cdot 10^{-5}$ (a = 120 km and b = 8 m) from the best fit of run-up distributions for the 1693 tsunami (Fig. 8a) obtained from inundation data using different Manning *n* values (Table 1). In order to account for uncertainties in the run-up evaluation, we calculate I_2 also using "a" and "b" values obtained by maximum (Fig. 8b) and minimum run-up (Fig. 8c) distributions, acquired from *n* = 0.07 and 0.03. This yields $I_2 = 7.33 \cdot 10^{-5}$ (a = 150 km and b = 11 m) and $I_2 = 4.1 \cdot 10^{-5}$ (a = 110 km and b =

4.5 m), respectively. These three I_2 values are comparable showing that, with similar lengths of affected coastline, the variation in the run-up values has negligible influence in the I_2 parameter. Thus, since the I_2 values are all smaller than 10^{-4}, the 1693 tsunami source was most likely a seismic dislocation.

In order to model different source types, Okal and Synolakis (2004) also considered two other dimensionless quantities I_1 and I_3. I_1 scales the maximum run-up on the beach to the amplitude of seismic slip on the fault:

$$I_1 = b/\Delta u$$

where "b" is the maximum run-up and Δu is the average coseismic slip on the fault.

Additionally, because a submarine landslide produces a deformation field that is dipolar in nature, with the surface of the sea featuring a negative depression (trough) and a positive elevation (hump), I_3 scales the maximum run-up on the beach to the amplitude of the initial depression on the sea surface:

$$I_3 = - b/\eta_-$$

where "b" is the maximum run-up and η_- is the amplitude of the initial depression on the sea surface.

In order to compute I_1 and I_3, the slip Δu and depression η_- are inferred from published values. For the 1908 tsunami source we use $\Delta u = 2.07 \pm 0.83$ m (Pino et al., 2000) and for the 1693 tsunami source $\Delta u = 2$ m (Gutscher et al., 2006). To compute I_3 for the 6 Feb 1783 tsunami source, we used an amplitude of depression $\eta_- = 10\text{-}20$ m (Bosman et al., 2006).

Okal and Synolakis (2004) demonstrated, using a comparison of I_2 vs. I_1 or I_3 (Fig. 9) that modeled tsunamis generated from either seismic dislocations or landslides are distributed in two different groups. Furthermore, among the worldwide events used by the authors, two of them stand out as clearly anomalous (inverted grey triangles in

Fig. 9), in excess of the range obtained for dislocations (black triangles in Fig. 9), confirming that these two tsunamis are due to an underwater landslide. We plotted the I_1 or I_3 vs. I_2 values obtained from our analysis onto the Okal and Synolakis (2004) graph (Fig. 9). The I_1 and I_2 values associated with both the 1908 and 1693 tsunamis fall in the range of earthquake generated tsunamis (diamonds and empty triangles in Fig. 9). The I_3 vs. I_2 1783 values (squares in Fig. 9) are clearly in the range of landslides. This confirms that both the 1908 and 1693 tsunamis were generated by a seismic dislocation, while the 1783 tsunami was generated by a landslide (Fig. 9).

What seems to make the critical difference in the way tsunamis from the two types of sources are manifest is the extent of the coastline affected. A substantially larger amount of coast is affected for a tectonic displacement than for a landslide source. In addition, the variation in run-up heights along the coast is also different. Seismic displacement yields a greater variability in tsunami run-ups than does a landslide.

5. Conclusion

Historical inundation and run-up data for several historical tsunamis that affected southern Calabria and eastern Sicily were applied to a methodology developed by Okal and Synolakis (2004) to evaluate their sources. Tsunamis generated on 28 December1908 and 6 February 1783, for which there is already agreement among researchers regarding the origin, were evaluated in order to test the methodology. We then applied this method to the 11 January 1693 tsunami, for which the causative source, fault- or landslide-generated, is equivocal (Tinti and Armigliato, 2003; Tinti et al., 2007).

As part of this analysis, we estimated run-up at individual locations for each tsunami. We used direct observations of run-up and inundation distance for the 1908 event. We were able to reconstruct run-up heights for some of the previous events using relations between inundation and run-up height. We calculated the dimensionless parameter I_2, which is the ratio of the maximum run-up to its lateral extent along the shore. I_2 values less than 10^{-4} are likely associated with a seismic source. I_2 values greater than 10^{-4} are most likely generated by a submarine landslide source (Okal and Synolakis, 2004). We estimated an I_2 value smaller than 10^{-4} for the 1908 and 1693 tsunamis, indicating they were related to a seismic dislocation source. Conversely, for the 1783 tsunami, I_2 is larger than 10^{-4} indicating its source was probably a landslide. Contemporary descriptions of the 1783 tsunami indicate that it was in all probability related to a large earthquake-induced rock-fall and submarine slide at the southwestern side of Scilla beach. This interpretation was recently supported by offshore geophysical investigations depicting a large submarine landslide with a prominent scar located immediately off-shore from the subaerial slide (Bosman et al., 2006; Bozzano et al., 2006).

Based on the successful application of the Okal and Synolakis (2004) methodology to the 1908 and 1783 events, we consider results obtained for the 1693 tsunami source, which suggest an earthquake dislocation origin, to be reasonable. This conclusion does not rule out the possibility that localized, earthquake-induced underwater landslides may have occurred. Indeed, a recent attempt at landslide modeling performed by Tinti et al. (2007) shows run-up peaks of up to 5 m along a 20 km long stretch of shoreline near Augusta. A landslide source does not explain the occurrence of inundation from the Aeolian Islands to the old Port of Marina di Ragusa (Mazzarelli in Fig. 2) reported by historical accounts, but may suggest a possible superposition of effects due to both fault dislocation and landslide.

Although uncertainties in the estimate of individual run-up amplitudes exist, the strength of this approach is evident in the overall analysis of the run-up distribution. The length of the inundated coast seems to be the key factor in discriminating the tsunami source: landslide sources concentrate large run-ups over relatively limited stretches of coastline, whereas seismic dislocations can affect much longer stretches of the coast. This was also shown recently by numerical modeling of tsunamis generated by earthquakes and landslides in the western Gulf of Corinth, where tsunamis caused by dislocation propagated over a wider area with respect to those caused by submarine landslides (Tinti et al., 2006).

Data and Resources

DISS Working Group (2006). Database of Individual Seismogenic Sources (DISS), Version 3.0.2: A compilation of potential sources for earthquakes larger than M 5.5 in Italy and surrounding areas. http://www.ingv.it/DISS/, © INGV 2006

Working Group CPTI (2004). Catalogo Parametrico dei Terremoti Italiani, versione 2004 (CPTI04). INGV, Bologna. http://emidius.mi.ingv.it/CPTI/

Acknowledgments

This study was funded by the Italian Dipartimento della Protezione Civile in the framework of the 2004-2006 agreement with Istituto Nazionale di Geofisica e Vulcanologia - INGV. We wish to thank Ted Bryant, editor Mark Hemphill-Haley and an anonymous reviewer, whose criticisms and suggestions helped to substantially improve the original manuscript.

References

Anonymous (1693). Vera Relazione di quello che è successo nell'ultimo terremoto in Sicilia. Toulon.

ASV (1693). Archivio Segreto Vaticano, Segreteria di Stato, Inquisizione Malta, vol. 44, cc. 11-16, Relazione dell'Inquisitore di Malta F. d'Acquaviva al Segretario di Stato Cardinale Spada sui danni causati a Malta e in Sicilia dal terremoto dell'11 gennaio 1693. Malta.

Argnani, A., and C. Bonazzi (2005). Malta Escarpment fault zone offshore eastern Sicily: Pliocene-Quaternary tectonic evolution based on new multichannel seismic data. Tectonics **24** (4): Art. No. TC4009, 1-12.

Azzaro, R., and M.S. Barbano (2000). Analysis of seismicity of Southeastern Sicily: a proposed tectonic interpretation. Ann. Geofis. **43**, 171-188.

Baratta, M. (1901). I terremoti d'Italia. Saggio di storia, geografia e bibliografia sismica italiana, 950 pp., Torino.

Baratta, M. (1910). La catastrofe sismica calabro-messinese (28 Dicembre 1908). Relazione alla Soc. Geogr. Ital., 426 pp. Roma.

Barbano, M.S., and M. Cosentino (1981). Il terremoto siciliano dell'11 Gennaio 1693. Rend. Soc. Geol. It. **4**, 517-522.

Basili, R., Valensise, G., Vannoli, P., Burrato, P., Fracassi, U., Mariano, Sofia, Monica Tiberti, M., Boschi, E. (2008). The Database of Individual Seismogenic Sources (DISS), version 3: summarizing 20 years of research on Italy's earthquake geology. Tectonophysics, doi:10.1016/j.tecto.2007.04.014.

Billi, A., Funiciello, R., Minelli, L., Faccenna, C., Neri, G., Orecchio, B., and Presti, D. (2008). On cause of the 1908 Messina tsunami, Southern Italy. Geophys. Res. Lett., **35**, L06301, doi:10.1029/2008GL033251

Boccone, P. (1697). Intorno il terremoto della Sicilia seguito l'anno 1693. Museo di Fisica, 31 pp., Venezia.

Boschi, E., E. Guidoboni, G. Ferrari, P. Gasperini, D. Mariotti, and G. Valensise (2000). Catalogue of Strong Italian Earthquakes from 461 a.C. to 1997. Ann. Geof. **43**, 609-868 and CD-ROM.

Bosman, A., F. Bozzano, F.L. Chiocci, and P. Mazzanti (2006). The 1783 Scilla tsunami: evidences of a submarine landslide as a possible (con?)cause. Geophys. Res. Abstracts, Vol. **8**, 10558, EGU 2006.

Bottone, D. (1718). De immani Trinacriae terraemotu. Idea historico-physica, in qua non solum telluris concussiones transactae recensentur, sed novissimae anni 1717. Messina.

Bozzano, F., F.L. Chiocci, P. Mazzanti, A. Bosman, D. Casalbore, R. Giuliani, S. Martino, A. Prestininzi, and G. Scarascia Mugnozza (2006). Subaerial and submarine characterization of the landslide responsible for the 1783 Scilla tsunami. Geophys. Res. Abstracts, Vol. **8**, 10422, EGU 2006.

Camassi, R., and M. Stucchi (1997). NT4.1, un catalogo parametrico di terremoti di area italiana al di sopra della soglia del danno. GNDT, Rapporto Interno, 95 pp. Milano.

Campis, P. (1694). Disegno historico o siano l'abbozzate historiae della nobile e fidelissima città di Lipari (ms. 1694), a cura di G. Iacolino, Lipari 1991.

D'Addezio, G., and G. Valensise (1991). Metodologie per l'individuazione della struttura sismogenetica responsabile del terremoto del 13 Dicembre 1990, in: Boschi E., Basili, A. (Eds), Contributi allo studio del terremoto della Sicilia orientale del 13 dicembre 1990, I.N.G. 537, 115-125.

De Rossi, M.S. (1889). Documenti raccolti dal defunto Conte Antonio Malvasia per la storia dei terremoti ed eruzioni vulcaniche massime d'Italia, in: Memorie della Pontificia Accademia dei Nuovi Lincei, vol.5, pp.169-289. Roma.

Galli, P., and P. Bosi (2002). Paleoseismology along the Cittanova fault. Implications for seismotectonics and earthquake reccurrence in Calabria (southern Italy). J. Geophys. Res. **107**, 83, 1-18, NO. B3, 10.1029/2001JB000234.

Ghisetti, F. (1992). Fault parameters in the Messina Straits (southern Italy) and relations with the seismogenetic source. Tectonophysics **210,** 117-133.

Graziani, L., A. Maramai, and S. Tinti (2006). A revision of the 1783–1784 Calabrian (southern Italy) tsunamis. Nat. Hazards Earth Syst. Sci. **6**, 1053–1060.

Gutscher, M.A., J. Roger, M.A. Baptista, J.M. Mirando, and S. Tinti (2006). Source of the 1693 Catania earthquake and tsunami (southern Italy): new evidence from tsunami modelling of a locked subduction fault plane. Geophys. Res. Lett. **33**, L08309, doi:10.1029/2005GL025442.

Hills, J.G., and C.L. Mader (1997). Tsunami produced by the impact of small asteroids. Ann. NY Acad. Sci. **882**, 381-394.

Jacques, E., C. Monaco, P. Tapponier, L. Tortorici, and T. Winter (2001). Faulting and earthquake triggering during the 1783 Calabria seismic sequence. Geophys. J. Int. **147**, 499-516.

Mercalli, G. (1897). I terremoti della Calabria meridionale e del messinese, in: Memorie della Società Italiana delle Scienze (detta dei XL), s. III, tomo 11, pp. 117-266. Roma.

Mercalli, G. (1909). Contributo allo studio del terremoto calabro-messinese del 28 dicembre 1908, in: Atti del Regio Istituto di Incoraggiamento di Napoli, s. VI, vol. 7, pp. 249-292. Napoli.

Minasi, G. (1785). Continuazione ed appendice sopra i tremuoti descritti nella relazione colla data di Scilla de 30 settembre 1783 con altro che accadde in progresso. Messina

Monaco, C., and L. Tortorici (2000). Active faulting in the Calabrian arc and eastern Sicily. J. Geodyn. **29,** 407-424.

Mongitore, A. (1743). Istoria cronologica de' terremoti di Sicilia, in: Id., Della Sicilia ricercata nelle cose più memorabili, tomo 2, pp. 345-445, Palermo.

Okal, E.A., and C.E. Synolakis (2004). Source discriminants for near-field tsunamis. Geophys. J. Int. **158**, 899-912.

Perrey, A. (1848). Mémoire sur les tremblements de terre de la penisule italique, in: Mémoires Couronnés et Mémoires des Savants Étrangers de l'Académie Royale de Belgique, tomo 22 (1846-47), pp. 1-144.

Piatanesi, A., and S. Tinti (1998). A revision of the 1693 eastern Sicily earthquake and tsunami. J. Geophys. Res. **103**, 2749-2758.

Piatanesi, A., S. Tinti, and E. Bortolucci (1999). Finite-Element Simulation of the 28 December 1908 Messina Straits (Southern Italy) tsunami. Phys. Chem. Earth (A) **24**, 2, 145-150.

Pino, N.A., D. Giardini, and E. Boschi (2000). The December 28, 1908, Messina Straits, southern Italy, earthquake: Waveform modelling of regional seismograms. J. Geophys. Res. **105**, NO B11, 25473-25492.

Platania, G. (1909). Il Maremoto dello Stretto di Messina del 28 dicembre 1908. Boll. Soc. Sismol. Ital. **13**, 369-458. Modena.

Sabatini, V. (1910). Contributo allo studio dei terremoti calabresi. Tip. Bertero. Roma.

Sarconi, M. (1784). Istoria de’ fenomeni del tremoto avvenuto nelle Calabrie, e nel Valdemone nell’anno 1783 posta in luce dalla Reale Accademia delle Scienze, e delle Belle Lettere di Napoli. Napoli.

Sirovich, L., and F. Pettenati (1999). Seismotectonic outline of South-Eastern Sicily: an evaluation of available options for the earthquake fault rupture scenario. J. Seismol. **3**, 213-233.

Spallanzani, L. (1795). Viaggi alle Due Sicilie e in alcune parti dell'Appennino. Tomo IV, 145-155. Pavia

Tinti, S., and A. Artigliato (2003). The use of scenarios to evaluate the tsunami impact in southern Italy. Mar. Geol. **199**, 221-243.

Tinti S., A. Maramai, and L. Graziani (2004). The new catalogue of Italian tsunamis, Nat. Hazards, **33**, 439-465.

Tinti, S., A. Armigliato, L. Bressan, S. Gallazzi, A. Manucci, and G. Pagnoni (2006). Simulazioni numeriche di maremoti generati da terremoti e frane nella parte occidentale del Golfo di Corinto (Grecia). Extended abstract, 25th Convegno Nazionale GNGTS, 41-42.

Tinti, S., A. Argnani, F. Zaniboni, G. Pagnoni, and A. Armigliato (2007). Tsunamigenic potential of recently mapped submarine mass movements offshore eastern Sicily (Italy): numerical simulations and implications for the 1693 tsunami. Abstract n. 8235, IUGG XXIV General Assembly.

Valensise, G. and D. Pantosti (1992). A 125 Kyr-long geological record of seismic source repeatability: in the Messina Straits (southern Italy) and the 1908 earthquake, Terra Nova **44**, 472-483.

Vivenzio, G. (1783). Istoria e teoria dè tremuoti in generale ed in particolare di quelli della Calabria, e di Messina del MDCCLXXXIII. Napoli.

Figure captions

Fig. 1 - Historical earthquakes accompanied by tsunamis; epicentres (empty circles) from the CPTI4 catalogue (Working group, 2004) and (filled circles) from the NT4.1 catalogue (Camassi and Stucchi, 1997). Possible source proposed for the 6 Feb 1783 earthquake: SF = Scilla fault (Jacques et al., 2001); the 28 Dec 1908 earthquake: M1 = Straits of Messina fault (Jacques et al., 2001) and M2 = Straits of Messina fault (DISS Working Group, 2006 and references therein); the 11 Jan 1693 earthquake: L1-L2 faults associated with the Scordia-Lentini graben (D'Addezio and Valensise, 1991); SL = Scicli Line (Sirovich and Pettenati, 1999); ME = Malta Escarpment (Azzaro and Barbano, 2000; Jacques et al., 2001); RF = Ragusa fault (DISS Working Group, 2006); SZ = subduction zone fault (Gutscher et al., 2006).

Fig. 2 – 11 Jan 1693 tsunami historical run-up and inundation observations (Boccone, 1697; Mongitore, 1743); computed run-up values are based on Hills and Mader (1997) relations between inundation and run-up: values in grey represent run-ups computed using the n values reported in Table 1; values in parentheses represent minimum and maximum run-up computed using $n = 0.03$ and 0.07, respectively (see text).

Fig. 3 - 6 Feb 1783 tsunami historical run-up and inundation values (Vivenzio, 1783; Sarconi, 1784); computed run-ups are based on the Hills and Mader (1997) relations between inundation and run-up: values in grey represent run-ups computed using the n values reported in Table 1; values in parentheses represent minimum and maximum possible run-up computed using $n = 0.03$ and 0.07, respectively (see text).

Fig. 4 - Data based on historical reports of the 28 Dec 1908 tsunami (Platania, 1909; Baratta, 1910): observed run-up and inundation values along the Calabrian (a, b) and Sicilian (c, d) coasts.

Fig. 5 - Tsunami run-up heights versus maximum landward inundation for different land roughness, based on Hills and Mader (1997). Black diamonds represent observed 1908 data. Grey triangles are the 1908 run-ups predicted from inundation using different Manning *n* values for each site (see text).

Fig. 6 - Run-up distributions for the 28 Dec 1908 tsunami along different idealized coastline profiles for which strike is depicted on the upper right corner inset maps. Star represents the closest point of the profile to the source location. The curves are the best-fit of the Okal and Synolakis (2004) equation (2); the “a”, “b”, “c” parameters are the relative values of best-fit curves obtained using: (a) observed run-up data in the Calabrian coast, (b) observed run-up data in the Sicilian coast, (c) observed run-up data from both the Calabria and Sicilian coasts.

Fig. 7 - Run-up distributions for the 6 Feb 1783 tsunami obtained using observed and computed run-up values, along two idealized coastline profiles depicted in upper right corner inset maps (N10°E and N35°E strikes). The star represents the closest point of the profile to the source location. The curves are best-fit to equation (2) (Okal and Synolakis,2004); the “a”, “b”, “c” parameters are the relative values of each best-fit curve. The left panels show the best-fit curves obtained plotting on the N10°E profile: (a) run-ups computed using different Manning *n* values in Table 1; (b) maximum run-ups; (c) minimum run-ups. The right panels illustrate the obtained best-fit curves plotted

on the N35°E profile: (d) run-ups computed using different Manning *n* values in Table 1; (e) maximum run-ups; (f) minimum run-ups.

Fig. 8 - Run-up distributions for the 11 Jan 1693 tsunami obtained using observed and computed data plotted along an idealized coastline profile whose strike (N10°E) is depicted on the upper right corner inset maps. The star represents the closest point of the profile to the source location. The curves are the best fit of Okal and Synolakis (2004) equation (2); the “a”, “b”, “c” parameters are the relative values of best-fit curves obtained using: (a) run-ups computed using different Manning *n* values in Table 1; (b) maximum run-ups; (c) minimum run-up values.

Fig. 9 - I_1 or I_3 *vs.* I_2 adimensional parameters obtained by Okal and Synolakis (2004): black dots represent dislocation models, grey dots represent landslide models, whereas black and grey triangles refer to worldwide observed dislocation and landslide tsunami data, respectively. The two distinct boxes segregate dislocation (black box) from landslide sources (dashed grey box). Results from the present work are also plotted. Diamonds show results for 1908 tsunami using I_2 obtained from “a” and “b” values of Fig. 6, and I_1 obtained from average coseismic slip in the range $\Delta u = 2.07 \pm 0.83$ m (Pino et al., 2000). The biggest triangles show results for 1693 tsunami using I_2 obtained from “a” and “b” values of Fig. 8 and I_1 obtained from $\Delta u = 2$ m (Gutscher et al., 2006). Squares show results for the 1783 tsunami, using I_2 obtained from “a” and “b” values of Fig. 7 and I_3 obtained from the average amplitude of depression $\eta_- = 10\text{-}20$ m (Bosman et al., 2006).

Table 1. Manning *n* values at single site along the coast used to predict run-ups for the 11 Jan 1693 and 6 Feb 1783 events (grey values in Figs. 2 and 3) from observed inundations. The *n* values are obtained by observed 1908 run-ups and inundations (Fig. 5).

Table 1

Location	Estimated Manning *n* values
Messina	$n = 0.07$
Giardini	$n = 0.04$
Mascali	$n = 0.03$
Catania	$n = 0.05$
Augusta	$n = 0.07$
Siracusa	$n = 0.07$
Mazzarelli	$n = 0.07$
Scilla	$n = 0.04$
Marina di Scilla	$n = 0.07$
Cannitello	$n = 0.07$
Catona	$n = 0.05$
Reggio Calabria	$n = 0.07$
Torre Faro	$n = 0.07$

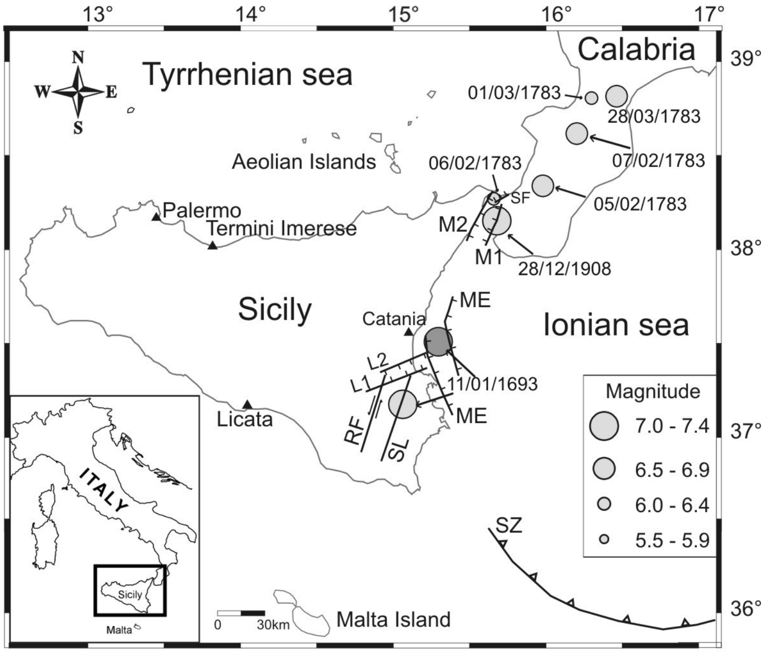
13°
14°
15°
16°
17°
39°
38°
37°
36°
Calabria
Tyrrhenian sea
N
W
E
S
01/03/1783
28/03/1783
07/02/1783
Aeolian Islands
06/02/1783
05/02/1783
SF
Palermo
Termini Imerese
M2
M1
28/12/1908
Sicily
ME
Catania
Ionian sea
L2
L1
11/01/1693
RF
SL
ME
Licata
ITALY
Sicily
Malta
Magnitude
7.0 - 7.4
6.5 - 6.9
6.0 - 6.4
5.5 - 5.9
SZ
0
30km
Malta Island
Fig.1

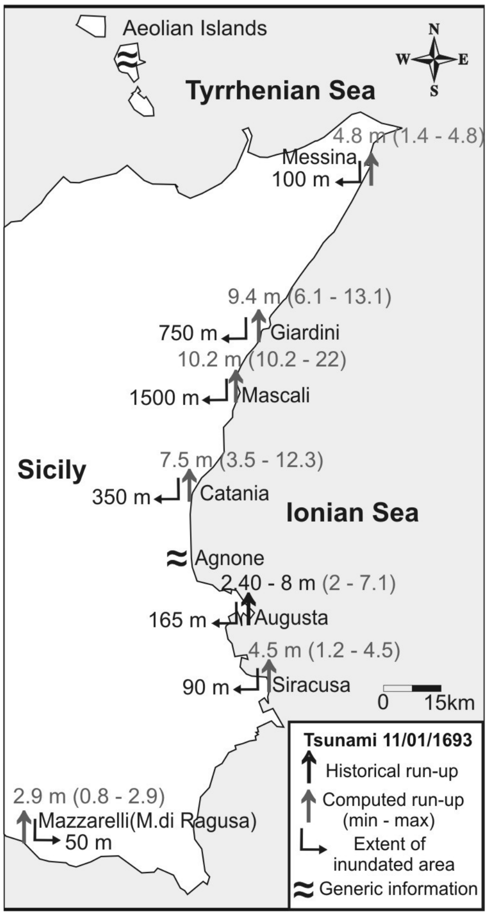
Aeolian Islands
N
W
E
S
Tyrrhenian Sea
4.8 m (1.4 - 4.8)
Messina
100 m
9.4 m (6.1 - 13.1)
750 m
Giardini
10.2 m (10.2 - 22)
1500 m
Mascali
Sicily
7.5 m (3.5 - 12.3)
350 m
Catania
Ionian Sea
Agnone
2.40 - 8 m (2 - 7.1)
165 m
Augusta
4.5 m (1.2 - 4.5)
90 m
Siracusa
0
15km
2.9 m (0.8 - 2.9)
Mazzarelli(M.di Ragusa)
50 m
Tsunami 11/01/1693
Historical run-up
Computed run-up (min - max)
Extent of inundated area
Generic information
Fig.2

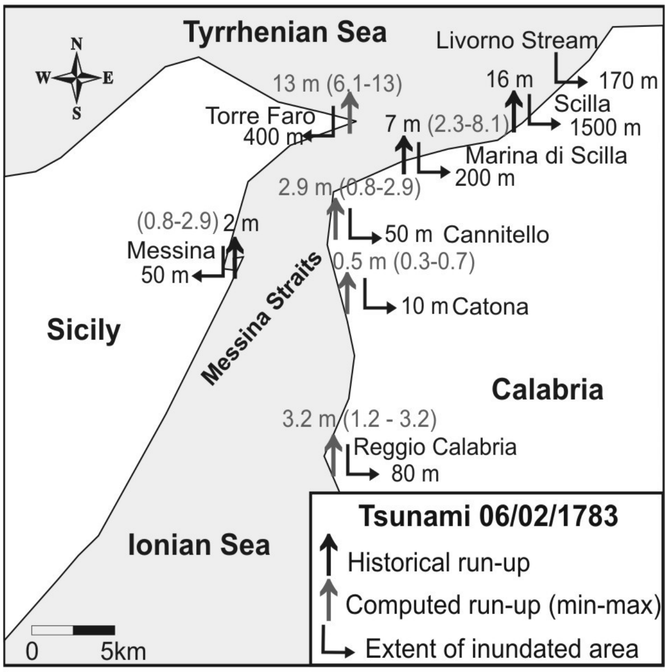
Tyrrhenian Sea
N
W
E
S
Livorno Stream
13 m (6.1-13)
16 m
170 m
Scilla
1500 m
Torre Faro
400 m
7 m (2.3-8.1)
Marina di Scilla
200 m
2.9 m (0.8-2.9)
(0.8-2.9) 2 m
Messina
50 m
50 m Cannitello
0.5 m (0.3-0.7)
10 m Catona
Sicily
Messina Straits
Calabria
3.2 m (1.2 - 3.2)
Reggio Calabria
80 m
Ionian Sea
Tsunami 06/02/1783
Historical run-up
Computed run-up (min-max)
Extent of inundated area
0
5km

Fig.3

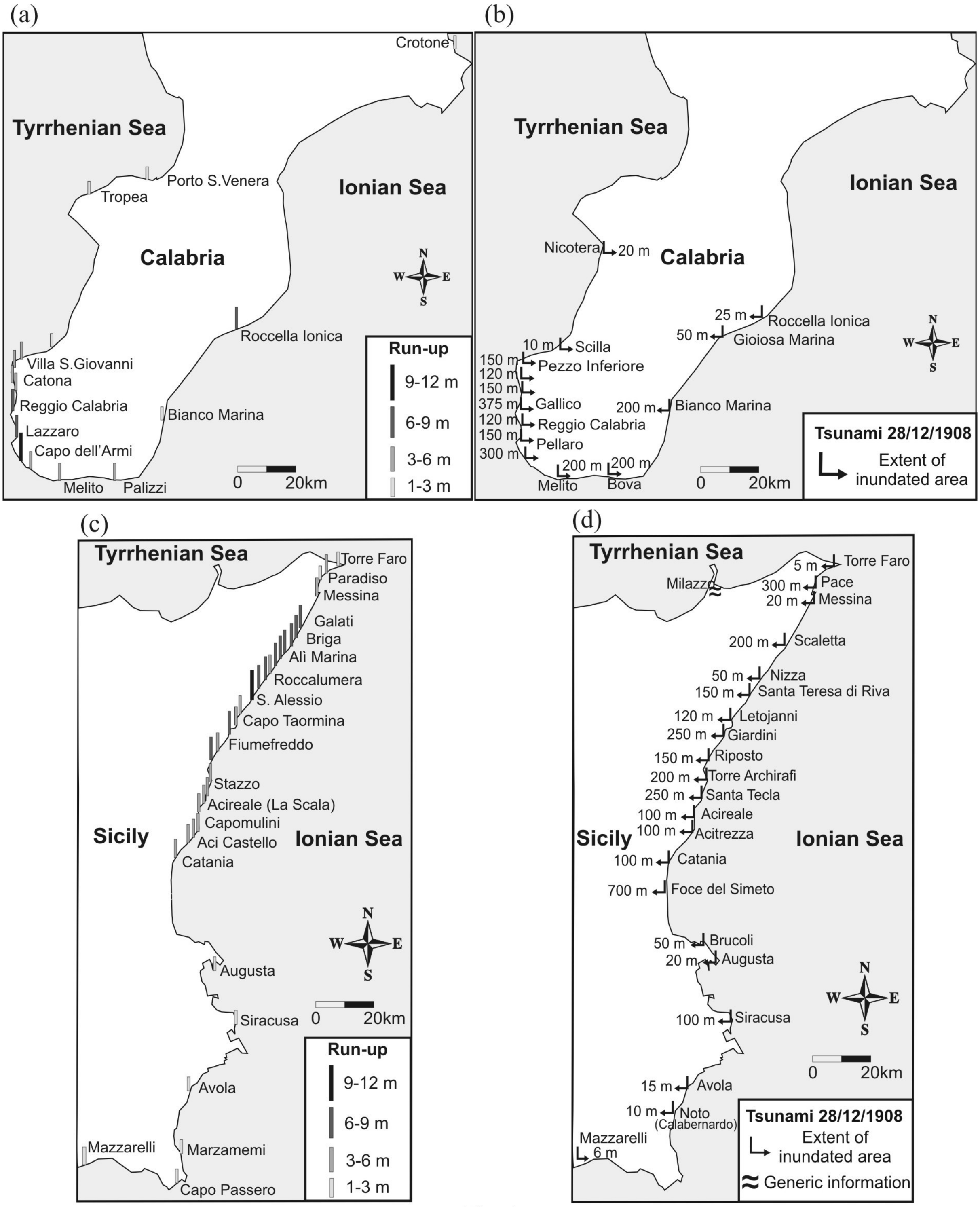
(a)
Crotone
Tyrrhenian Sea
Porto S.Venera
Tropea
Ionian Sea
Calabria
Roccella Ionica
Villa S.Giovanni
Catona
Reggio Calabria
Bianco Marina
Lazzaro
Capo dell'Armi
Melito
Palizzi
0
20km
Run-up
9-12 m
6-9 m
3-6 m
1-3 m
(b)
Tyrrhenian Sea
Ionian Sea
Nicotera
20 m
Calabria
25 m
Roccella Ionica
50 m
Gioiosa Marina
10 m
Scilla
150 m
Pezzo Inferiore
120 m
150 m
375 m
Gallico
200 m
Bianco Marina
120 m
Reggio Calabria
150 m
Pellaro
300 m
200 m
200 m
Melito
Bova
0
20km
Tsunami 28/12/1908
Extent of inundated area
(c)
Tyrrhenian Sea
Torre Faro
Paradiso
Messina
Galati
Briga
Alì Marina
Roccalumera
S. Alessio
Capo Taormina
Fiumefreddo
Stazzo
Acireale (La Scala)
Capomulini
Sicily
Aci Castello
Ionian Sea
Catania
Augusta
Siracusa
0
20km
Run-up
9-12 m
Avola
6-9 m
Mazzarelli
Marzamemi
3-6 m
Capo Passero
1-3 m
(d)
Tyrrhenian Sea
5 m
Torre Faro
Milazzo
300 m
Pace
20 m
Messina
200 m
Scaletta
50 m
Nizza
150 m
Santa Teresa di Riva
120 m
Letojanni
250 m
Giardini
150 m
Riposto
200 m
Torre Archirafi
250 m
Santa Tecla
100 m
Acireale
100 m
Acitrezza
Sicily
Ionian Sea
100 m
Catania
700 m
Foce del Simeto
50 m
Brucoli
20 m
Augusta
100 m
Siracusa
0
20km
15 m
Avola
10 m
Noto
(Calabernardo)
Tsunami 28/12/1908
Mazzarelli
6 m
Extent of inundated area
Generic information

Fig.4

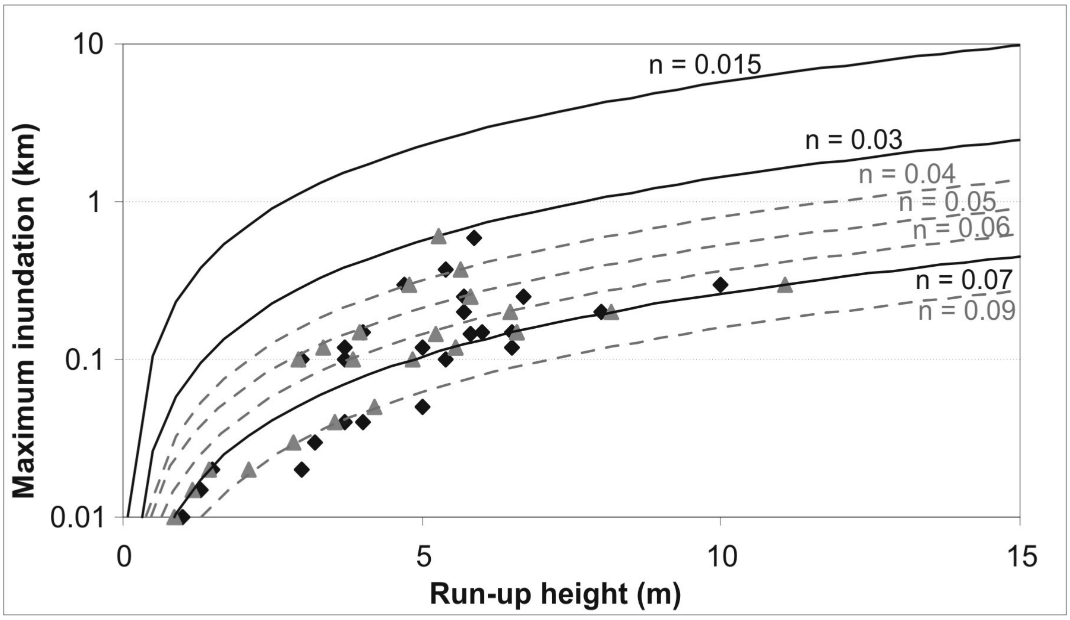
n = 0.015
n = 0.03
n = 0.04
n = 0.05
n = 0.06
n = 0.07
n = 0.09
Maximum inundation (km)
10
1
0.1
0.01
0
5
10
15
Run-up height (m)

Fig.5

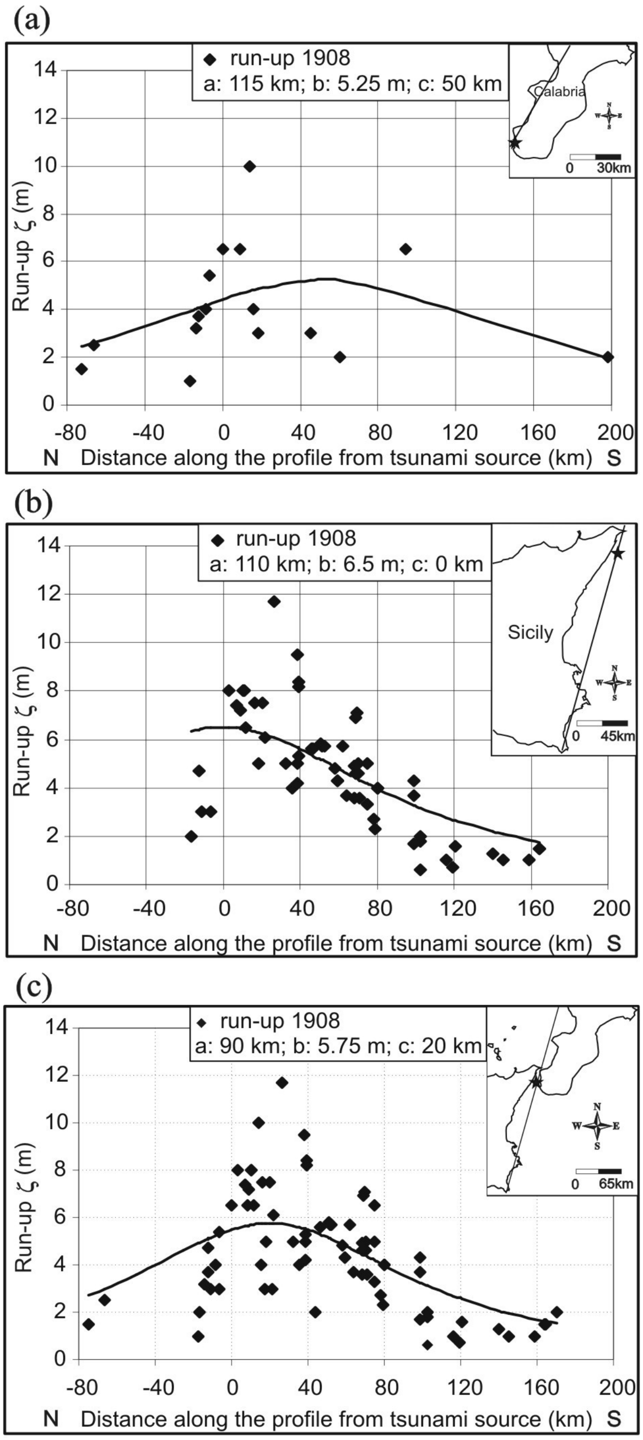

(a)
run-up 1908
a: 115 km; b: 5.25 m; c: 50 km
Calabria
0 30km
Run-up ζ (m)
N Distance along the profile from tsunami source (km) S
(b)
run-up 1908
a: 110 km; b: 6.5 m; c: 0 km
Sicily
0 45km
Run-up ζ (m)
N Distance along the profile from tsunami source (km) S
(c)
run-up 1908
a: 90 km; b: 5.75 m; c: 20 km
0 65km
Run-up ζ (m)
N Distance along the profile from tsunami source (km) S

Fig.6

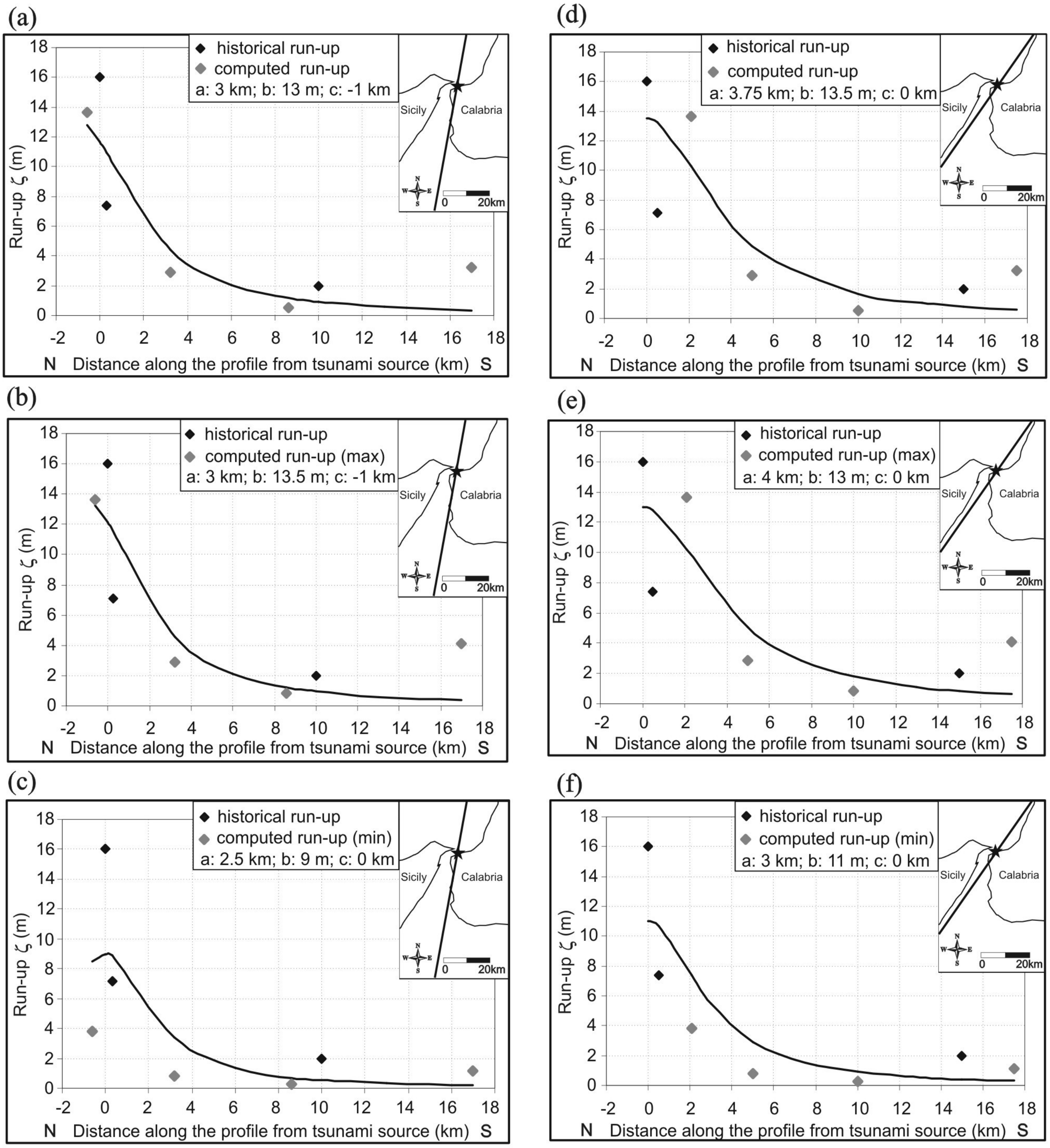
(a)
historical run-up
computed run-up
a: 3 km; b: 13 m; c: -1 km
(b)
historical run-up
computed run-up (max)
a: 3 km; b: 13.5 m; c: -1 km
(c)
historical run-up
computed run-up (min)
a: 2.5 km; b: 9 m; c: 0 km
(d)
historical run-up
computed run-up
a: 3.75 km; b: 13.5 m; c: 0 km
(e)
historical run-up
computed run-up (max)
a: 4 km; b: 13 m; c: 0 km
(f)
historical run-up
computed run-up (min)
a: 3 km; b: 11 m; c: 0 km
Run-up ζ (m)
N Distance along the profile from tsunami source (km) S
Sicily
Calabria
0 20km

Fig.7

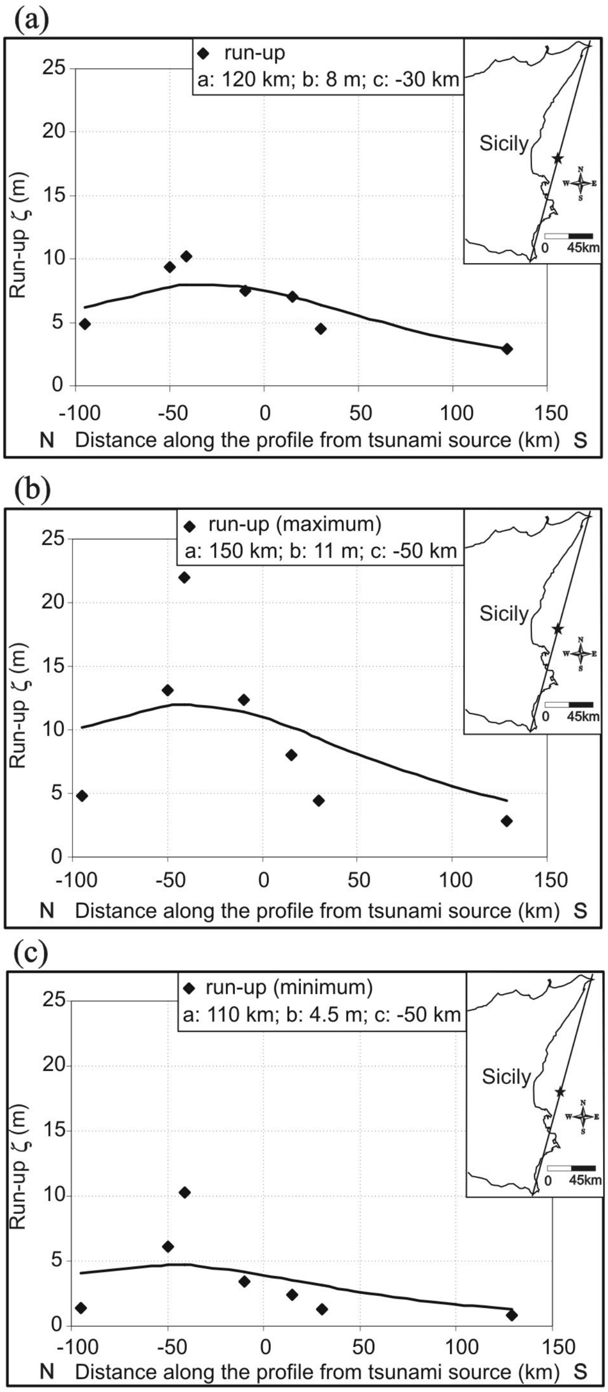

(a)
run-up
a: 120 km; b: 8 m; c: -30 km
Sicily
0
45km
Run-up ζ (m)
N
Distance along the profile from tsunami source (km)
S
(b)
run-up (maximum)
a: 150 km; b: 11 m; c: -50 km
Sicily
0
45km
Run-up ζ (m)
N
Distance along the profile from tsunami source (km)
S
(c)
run-up (minimum)
a: 110 km; b: 4.5 m; c: -50 km
Sicily
0
45km
Run-up ζ (m)
N
Distance along the profile from tsunami source (km)
S

Fig.8

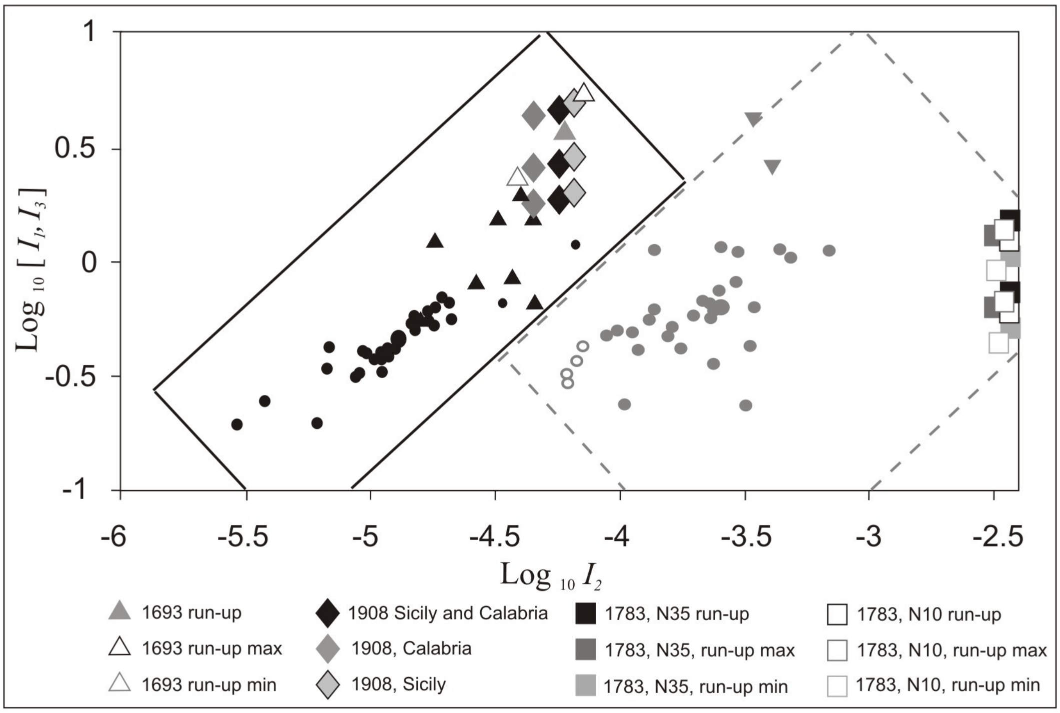

1
0.5
0
-0.5
-1
-6
-5.5
-5
-4.5
-4
-3.5
-3
-2.5
Log $_{10}$ [I_1, I_3]
Log $_{10}$ I_2
1693 run-up
1693 run-up max
1693 run-up min
1908 Sicily and Calabria
1908, Calabria
1908, Sicily
1783, N35 run-up
1783, N35, run-up max
1783, N35, run-up min
1783, N10 run-up
1783, N10, run-up max
1783, N10, run-up min

Fig.9